# BIOLOGICAL AND PHYSICOCHEMICAL PROPERTIES OF BOVINE SODIUM CASEINATE HYDROLYSATES OBTAINED BY A BACTERIAL PROTEASE PREPARATION

María Eugenia Hidalgo[a,b], Ana Paula Folmer Côrrea[c], Manuel Mancilla Canales[a,b], Daniel Joner Daroit[d], Adriano Brandelli[c]; Patricia Risso[a,b,e]

[a] Departamento de Química-Física, Facultad de Ciencias Bioquímicas y Farmacéuticas, Universidad Nacional de Rosario (UNR), Suipacha 531 (2000) Rosario, Santa Fe, Argentina

[b] Instituto de Física Rosario (IFIR-CONICET-UNR), 27 de Febrero 210 Bis (2000) Rosario, Santa Fe, Argentina

[c] Instituto de Ciência e Tecnologia de Alimentos (ICTA), Universidade Federal de Rio Grande do Sul (UFRGS), Av. Bento Gonçalves 9500, (91501-970) Porto Alegre, Brazil

[d] Universidade Federal da Fronteira Sul (UFFS), Campus Cerro Largo, 97900-000 Cerro Largo, RS, Brazil

[e] Facultad de Ciencias Veterinarias, Universidad Nacional de Rosario (UNR), Ovidio Lagos y Ruta 33 (2170) Casilda, Santa Fe, Argentina

maruhidalgo80@yahoo.com.ar

**Keywords:** *Bacillus sp.* P7; bovine sodium caseinate; hydrolysates; bioactivity; acid aggregation and gelation; microstructure

## Abstract

In this work, we aimed at the production of bovine sodium caseinate (NaCAS) hydrolysates by means of an extracellular protease from *Bacillus* sp. P7. Mass spectrometry was carried

out to evaluate peptide mass distribution and identified sequences of peptides with a signal/noise ratio higher than 10. Antioxidant and antimicrobial properties of hydrolysates were evaluated. An acid-induced aggregation process of the hydrolysates and their corresponding mixtures with NaCAS were also analyzed. The results showed that the enzymatic hydrolysis produced peptides, mostly lower than 3 kDa, with different bioactivities depending on the time of hydrolysis ($t_i$). These hydrolysates lost their ability to aggregate by addition of glucono-δ-lactone, and their incorporation into NaCAS solutions alter the kinetics of the process. Also, the degree of compactness of the NaCAS aggregates, estimated by the fractal dimension of aggregates, was not significantly altered by the incorporation of hydrolysates. However, at higher protein concentrations, when the decrease in pH leads to the formation of NaCAS acid gels, the presence of hydrolysates alters the microstructure and rheological behavior of these gels.

## 1. Introduction

Caseins (CN) are the main milk protein fraction (~ 80%) which occurs in micelles as large particles of colloidal size (Walstra, Jenness, & Badings, 1984). However, the micellar structure of CN is destroyed during the manufacture of sodium caseinate (NaCAS) (Mulvihill & Fox, 1989). NaCAS are extensively used in food industry because of their physicochemical, nutritional and functional properties, such as emulsifying and gelation capacities, thus contributing to food texture (Alvarez, Risso, Gatti, Burgos, & Suarez Sala, 2007; Nishinari, Zhang, & Ikeda, 2000).

A gel structure is formed during NaCAS acidification as a result of the dissociation and aggregation of CN fractions ($\alpha_{S1}$-, $\alpha_{S2}$-, β- and κ-). In the traditional process, NaCAS is

acidified by bacteria which ferment lactose to lactic acid. However, direct acidification achieved by the addition of a lactone, such as glucono-δ-lactone (GDL), has gained the attention of the food industry, since this process avoids potential complications related to starter bacteria (variable activity and variations with the type of culture used). In fact, the final pH of the system bears a direct relation to the amount of GDL added, whereas starter bacteria produce acid until they inhibit their own growth as pH becomes lower (Braga, Menossi, & Cunha, 2006; de Kruif, 1997).

The high growth in consumer demand for healthy and nutritional food products has encouraged the food industry to carry out an improvement in the development of natural and functional food ingredients and dietary supplements. In the primary sequence of proteins there are inactive peptides that could be released by enzymatic hydrolysis *in vivo* or *in vitro*. These peptides acquire different biological activities, such as opioid, antihypertensive, immunomodulatory, antibacterial and antioxidant activities, among others, with potential applications in food science and technology (FitzGerald, Murray, & Walsh, 2004; Haque & Chand, 2008; Phelan, Aherne, FitzGerald, & O'Brien, 2009; Sarmadi & Ismail, 2010; Silva & Malcata, 2005).

CN are considered important sources of bioactive peptides that could be released through different types of enzymatic hydrolysis using microbial or digestive enzymes (Korhonen, 2009; Silva, et al., 2005). Under moderate conditions of pH and temperature, it is possible to obtain components with biological activities that enhanced nutritional and functional properties such as gelation, emulsification and foam formation (Hartmann & Meisel, 2007; Silva, et al., 2005).

It is known that commercial proteases have been employed in the production of protein hydrolysates with bioactives properties such as antioxidant activity (Rival, Boeriu, &

Wichers, 2001; Saiga, Tanabe, & Nishimiura, 2003; Zhu, Zhou, & Qian, 2006). Microbial proteases are particularly interesting because of the high yield achieved during their production through well-established culture methods (Gupta, Beg, & Lorenz, 2002; Rao, Tanksale, Ghatge, & Deshpande, 1998). It have been reported that a proteolytic *Bacillus* sp. P7, isolated from the intestinal conduct of the Amazonian fish *Piaractus mesopotamicus*, produces high levels of extracellular proteases with biotechnological potential during submerged cultivations in inexpensive culture media (Corrêa, et al., 2011).

Enzymatic hydrolysis of proteins might be an alternative treatment to control the characteristics of acid-set gels and to confer desired rheological and organoleptic properties (Rabiey & Britten, 2009). The aims of this work were to obtain protein hydrolysates of bovine NaCAS with a protease preparation from *Bacillus* sp. P7, determine the peptide mass distribution, identified peptide sequences and evaluate their different bioactivities (antioxidant, antimicrobial, reducing and chelating power). Also, we the effects of the presence of these bioactive peptides on acid aggregation and gelation properties of NaCAS were studied.

## 2. Materials and Methods

### *2.1. Materials*

Bovine NaCAS powder, azocasein, the acidulant GDL, tris(hydroxymethyl)aminomethane (Tris), 8-anilino-1-naphthalenesulfonate (ANS) as ammonium salt; 2,4,6-trinitrobenzene sulfonic acid (TNBS); 2,2’-azino-bis-(3-ethylbenzothiazoline)-6-sulfonic acid (ABTS); ferrozine (3-(2-pyridyl)-5,6-bis(4-phenyl-sulfonic acid)-1,2,4-triazine) were commercially acquired from Sigma-Aldrich Co.

(Steinheim, Germany). Other chemicals employed were of analytical grade and were provided by Cicarelli SRL (San Lorenzo, Argentina).

*2.2. Bovine sodium caseinate (NaCAS) preparation*

NaCAS solutions were prepared by dissolving the commercial powder in distilled water. CN concentration was measured according to the Kuaye's method, which is based on the ability of strong alkaline solutions (0.25 mol $L^{-1}$ NaOH) to shift the spectrum of the amino acid tyrosine to higher wavelength values in the UV region (Kuaye, 1994). All the values obtained were the average of two determinations.

*2.3. Microorganism and protease preparation*

*Bacillus* sp. P7, which secretes the extracellular proteases, was maintained in Brain-Heart Infusion (BHI) agar plates. The strain was cultivated in feather meal broth (10 g $L^{-1}$ feather meal, 0.3 g $L^{-1}$ $Na_2HPO_4$, 0.4 g $L^{-1}$ $NaH_2PO_4$, 0.5 g $L^{-1}$ NaCl) for 48 h at 30 ºC in a rotary shaker (125 rpm) (Corrêa, Daroit, & Brandelli, 2010). Culture was centrifuged (10,000 × g for 15 min at 4 ºC) and the supernatant, which contained the extracellular proteolytic enzymes, was submitted to a partial purification.

*2.4. Protease partial purification*

The proteases were precipitated from culture supernatants by the gradual addition of solid ammonium sulfate to achieve 60% saturation, in an ice bath with gentle stirring. This mixture was allowed to stand for 1 h, centrifuged (10,000 × g for 15 min at 4 ºC), and the resulting pellet was dissolved in 20 x $10^{-3}$ mol $L^{-1}$ Tris-HCl buffer pH 8.0. The concentrated enzyme samples were applied to a Sephadex G-100 (Pharmacia Biotech,

Uppsala, Sweden) gel filtration column (25 × 0.5 cm) previously equilibrated with the above mentioned buffer, and elution was performed using the same buffer at a flow rate of 0.33 mL $min^{-1}$. Thirty fractions (1 mL) were collected and submitted to the proteolytic activity assay. Fractions showing enzymatic activity were pooled to will be use in NaCAS hydrolysis.

*2.5. Proteolytic activity assay*

Proteolytic activity was determined as described by Corzo-Martinez, Moreno, Villamiel and Harte (2010), using azocasein as substrate. The reaction mixture contained 100 μL enzyme preparation, 100 μL of 20 x $10^{-3}$ mol $L^{-1}$ Tris-HCl buffer pH 8.0, and 100 μL of 10 mg $mL^{-1}$ azocasein in the same buffer. The mixture was incubated at 37 ºC for 30 min, and the reaction was stopped by adding 500 μL of 0.10 g $mL^{-1}$ trichloroacetic acid (TCA). After centrifugation (10,000 × g for 5 min), 800 μL of the supernatant was mixed with 200 μL of 1.8 mol $L^{-1}$ NaOH, and the absorbance at 420 nm was measured (Corzo-Martínez, Moreno, Villamiel, & Harte, 2010). One unit of enzyme activity (U) was considered as the amount of enzyme that caused a change of 0.1 absorbance units under the above assay conditions. Fractions showing proteolytic activity on azocasein were pooled and employed as a P7 protease preparation (P7PP) for NaCAS hydrolysis.

*2.6. Hydrolysis of NaCAS*

Samples of 0.01 g $mL^{-1}$ of NaCAS in Tris-HCl buffer 20 x $10^{-3}$ mol $L^{-1}$, pH 8 were subjected to hydrolysis with the addition of 1 mL of P7PP (enzyme:substrate 1:50 ratio) at 45 °C. The hydrolysis reaction was stopped at different times ($t_i$; i = 0, 0.5, 1, 2, 3, 4, 6 and 7 h) by heating the samples to 100 ºC for 15 min. After centrifugation (10,000 × g for 15

142 min), the supernatants were recovered, lyophilized, and kept at -18 °C. Protein
143 concentration of the supernatants was measured as previously described (Kuaye, 1994).
144
145 *2.7. Degree of hydrolysis (DH)*
146 DH of NaCAS hydrolysates was determined by the TNBS method (Adler-Nissen,
147 1979). Protein hydrolysate samples (250 μL) were mixed with 2 mL phosphate buffer
148 (0.212 mol $L^{-1}$; pH 8.2) and 2 mL 1% TNBS, and incubated at 50 °C for 1 h. Then, 4 mL of
149 0.1 mol $L^{-1}$ HCl was added, and mixtures were maintained for 30 min at room temperature
150 before performing readings at 340 nm. Total amino groups in NaCAS was determined in a
151 sample (10 mg) which was completely hydrolyzed in 4 mL of 6 mol $L^{-1}$ HCl at 110 °C for
152 24 h (Li, Chen, Wang, Ji, & Wu, 2007).
153
154 *2.8. Urea-sodium dodecyl sulfate-polyacrylamide gel electrophoresis (Urea-SDS-*
155 *PAGE)*
156 qualitative composition of the hydrolysates was analysed by Urea-SDS-PAGE using a
157 vertical gel system, according to the method of Laemmli (Laemmli, 1970). The protein
158 bands were identified using commercial low molecular weight protein markers (Sigma
159 Chemical Co., Steinheim, Germany).
160
161 *2.9. Mass spectrometry*
162 Peptide mass distribution of hydrolysates was determined by MALDI-TOF-TOF mass
163 spectrometry, at the CEQUIBIEM proteomic facility from the Universidad de Buenos
164 Aires, using an Ultrafex II mass spectrometer (Bruker Corporation, USA). Peaks with a

signal/noise ratio higher than 10 were fragmented. The peptide sequences were predicted from the MS/MS data by using the proteomic tool Protein Prospector v.5.12.1 (http://prospector.ucsf.edu/prospector/mshome.htm) with the following searching conditions: NCBI 2013.6.17, taxonomy: *Bos taurus*, digestion: no enzyme, 200 ppm for parent ion tolerance, and 300 ppm for ion fragment tolerance.

### *2.10. Intrinsic fluorescence spectra*

Excitation and emission spectra of the hydrolysates (1 mg $mL^{-1}$) were obtained to detect any spectral shift and/or changes in the relative intensity of fluorescence (FI) in an Aminco Bowman Series 2 spectrofluorometer (Thermo Fisher Scientific, USA). The excitation wavelength ($\lambda_{exc}$) and the range of concentration with a negligible internal filter effect were previously determined. For spectral analysis and FI measurements samples (3 mL) were poured into a fluorescence cuvette (1 cm light path) and placed into a cuvette holder maintained at 35 °C. Values of FI (n = 2) were registered within the range of 300 to 420 nm using a $\lambda_{exc}$ of 286 nm.

### *2.11. Surface hydrophobicity ($S_0$)*

$S_0$ was estimated according to Kato and Nakai method (Kato & Nakai, 1980), using the ammonium salt of amphiphilic ANS as a fluorescent probe. The measurements were carried out using $\lambda_{exc}$ and emission wavelength ($\lambda_{em}$) set at 396 and 489 nm, respectively, at a constant temperature of 35 °C. Both wavelengths were previously obtained from emission and excitation spectra of protein-ANS mixtures.

Intensity of fluorescence of samples containing ANS and different concentrations of NaCAS hydrolysates ($FI_b$) as well as the intrinsic FI without ANS ($FI_p$) were determined (n = 3). The difference between $FI_b$ and $FI_p$ ($\Delta F$) was calculated, and $S_0$ was determined as the initial slope in the $\Delta F$ vs. protein concentration (g $mL^{-1}$) plot.

*2.12. NaCAS hydrolysates bioactivities in vitro*

*2.12.1. Antioxidant activity: ABTS method*

Scavenging of the ABTS radical was determined by the decolorization assay described by Re, Pellegrini, Proteggente, Pannala, Yang and Rice-Evans (1999). ABTS radical cation ($ABTS^{\bullet+}$) solution was prepared by reacting 7 x $10^{-3}$ mol $L^{-1}$ ABTS solution with 140 x $10^{-3}$ mol $L^{-1}$ $K_2SO_4$ (final concentration). This mixture was allowed to stand in the dark at room temperature for 12-16 h before use. For the assay, the $ABTS^{\bullet+}$ solution was diluted with 5 x $10^{-3}$ mol $L^{-1}$ phosphate buffered saline pH 7.0 (PBS) to an absorbance of 0.70 ± 0.02 at 734 nm. A 10 µL (15 mg $mL^{-1}$) of sample was mixed with 1mL of diluted $ABTS^{\bullet+}$ solution and absorbance at 734 nm was measured after 6 min. Trolox® was used as a reference standard. The percentage inhibition of absorbance at 734 nm was calculated and plotted as a function of the concentration of the reference antioxidant (Trolox®) (Re, et al., 1999).

*2.12.2. Metal chelating activity*

The chelating activity of $Fe^{2+}$ was measured using the method described by Chang, Wu and Chiang (2007), with slight modifications. One milliliter of sample (3.5 mg $mL^{-1}$) was mixed with 3.7 mL distilled water and then the mixture was reacted with 0.1 mL of 2 x

$10^{-3}$ mol $L^{-1}$ $FeSO_4$ ($Fe^{2+}$) and 0.2 mL of 5 x $10^{-3}$ mol $L^{-1}$ ferrozine. After 10 min, the absorbance was read at 562 nm. One milliliter of distilled water, instead of sample, was used as a control. Ethylene diamine tetra acetic acid (EDTA) 20 mg $mL^{-1}$ was used as standard (Chang, Wu, & Chiang, 2007). The results were expressed as $\text{Chelating activity } (\%) = \left[1 - \left(A/A_0\right)\right] \cdot 100$, where A is the absorbance of the test and $A_0$ is the absorbance of the control.

*2.12.3. Reducing power*

Reducing power of the hydrolysates was measured as previously described by Zhu, Zhou and Qian (2006). Samples (15 mg $mL^{-1}$) from each hydrolysis period were mixed with 2.5 mL phosphate buffer 0.2 mol $L^{-1}$ pH 6.6 and 2.5 mL potassium ferricyanide (10 mg $mL^{-1}$), and then the mixture was incubated at 50 ºC for 20 min. Then, 2.5 mL TCA (0.10 g $mL^{-1}$) was added and the mixture was centrifuged (3,000 × g for 10 min). One milliliter of supernatant was mixed with 2.5 mL distilled water and 0.2 mL ferric chloride (1 mg $mL^{-1}$), and the absorbance at 700 nm was measured. Higher absorbance of the reaction mixture indicated greater reducing power. Butylatedhydroxytoluene (BHT) at the same concentration of samples was used as a positive control (Zhu, et al., 2006).

*2.12.4. Antibacterial activity*

Antibacterial activity was determined according to Motta and Brandelli (2002) with modifications. The indicator strains tested were *Listeria monocytogenes* ATCC 15131, *Bacillus cereus* ATCC 9634, *Corynebacterium fimi* NCTC 7547, *Staphylococcus aureus* ATCC 1901, *Salmonella* Enteritidis ATCC 13076, and *Escherichia coli* ATCC 8739.

Indicator microorganisms, at a concentration of $10^8$ CFU $mL^{-1}$ in saline solution (NaCl 0.0085 g $mL^{-1}$), were inoculated with a swab onto BHI agar plates. Aliquots of 15 µL NaCAS hydrolysates (250 mg $mL^{-1}$) were spotted on the freshly prepared lawn of indicator strain, and plates were incubated at the optimal temperature for each test microorganism. Subsequently, zones of growth inhibition represented by clear haloes were measured and presented as inhibition zone (mm) (Motta & Brandelli, 2002).

*2.13. Determination of size variations of particles*

Changes in the average size of particles were followed by the dependence of turbidity ($\tau$) on wavelength ($\lambda$) of the suspensions, and determined as $\beta = 4.2 + \partial \log \tau / \partial \log \lambda$. $\beta$ is a parameter that has a direct relationship with the average size of the particles and can be used to easily detect and follow rapid size changes. It was obtained from the slope of log $\tau$ *vs* log $\lambda$ plots, in the 450-650 nm range, where the absorption owing to the protein chromophores is negligible allowing then to estimate $\tau$ as absorbance in 400-800 nm range (Camerini-Otero & Day, 1978). It has been shown that $\beta$, for a system of aggregating particles of the characteristics of caseinates tends, upon aggregation, towards an asymptotic value that can be considered as a fractal dimension ($D_f$) of the aggregates (Horne, 1987; Mancilla Canales, Hidalgo, Risso, & Alvarez, 2010; Risso, Relling, Armesto, Pires, & Gatti, 2007). $\tau$ was measured as absorbance using a Spekol 1200 spectrophotometer (Analytikjena, Belgium), with a diode arrangement. Determinations of $\beta$ were the average of at least duplicate measurements.

*2.14. Evaluation of acid aggregation process*

Kinetics of NaCAS or hydrolysates (5 mg $g^{-1}$) and NaCAS:hydrolysates mixtures (4:1) aggregation, induced by the acidification with GDL, was analyzed by measuring $\tau$ in the range of 450-650 nm, in a spectrophotometer with a thermostatized cell. The amount of GDL added was calculated using the relation R=GDL mass fraction/NaCAS mass fraction. R used for all these experiments was 0.5, at temperature of 35 °C.

Acidification was initiated by the addition of solid GDL to 6 g of different samples. Absorption spectra (450-650 nm) and absorbance at 650 nm ($A_{650}$) were registered as a function of time until a maximum and constant value of $A_{650}$ was reached; simultaneously, pH decrease was measured. The determinations were performed in duplicate and the values of parameter $\beta$ were calculated as above mentioned.

*2.15. Rheological properties of NaCAS:hydrolysate mixtures*

Gel formation of NaCAS:hydrolysate mixtures (30 mg $g^{-1}$ : 7.5 mg $g^{-1}$) was evaluated by oscillatory measurements using a stress and strain controlled rheometer (TA Instruments, AR G2 model, Brookfield Engineering Laboratories, Middleboro, USA). A cone geometry (diameter: 40 mm, cone angle: 2º, cone truncation: 55 mm) and a system of temperature control with a recirculating bath (Julabo model ACW 100, Seelbach, Alemania) connected to a Peltier plate were used for the measurements. Solid GDL was added in order to initiate the acid gelation at R=0.5. Measurements were performed every 20 s for 120 min with a constant oscillation stress of 0.1 Pa and a frequency of 0.1 Hz. The Lissajous figures at various times were plotted to make sure that the determinations of storage or elastic modulus (G′) and loss or viscous modulus (G″) were always obtained

within the linear viscoelastic region. The complex modulus (G*) and the pH were also monitored during acid gelation. Measurements were performed at least in triplicate.

### *2.16. Confocal laser scanning microscopy (CSLM)*

NaCAS:hydrolysate mixtures (30 mg $g^{-1}$ : 7.5 mg $g^{-1}$) were stained with Rhodamine B solution (2 x $10^{-3}$ mg $mL^{-1}$). An adequate amount of GDL (R = 0.5) was added to initiate the gelation process. Aliquots of 200 μL were immediately placed in compartments of LAB-TEK II cells (Thermo Scientific, USA). The gelation process was performed in an oven at (35 ± 1) °C, keeping the humidity controlled. Gels were observed with an 40x objective, a 2x zoom, by using an inverted scan confocal microscope NIKON TE2000E (Nikon Instruments Inc., USA), with handheld scanning, using 543 nm excitation He-Ne laser, 605-675 nm band emission. Acquired images were stored in tiff format for their further analysis.

In order to process the images obtained by CSLM and to obtain the texture parameters, specific programs were developed in Python language. The following three texture measures were used in this work: Shannon entropy (*S*), smoothness (*K*) and uniformity (*U*), given by:

$$S = -\sum_{i=0}^{L-1} p(N_i)\log_2\left(p(N_i)\right) \qquad U = \sum_{i=0}^{L-1} p^2(N_i) \qquad K = 1 - \frac{1}{1+\frac{\sigma^2(N)}{(L-1)^2}} \tag{1}$$

where $p(Ni)$ is the statistical sample frequency normalized from the grey scale, $L$ is the highest black level and $\sigma^2$ $(N)$ is the mean normalized grey-level variance which is particularly important in texture description because it is a measure of grey level contrast that may be used to establish descriptors of relative smoothness (Gonzalez & Woods,

2001). Previously, the color images were transformed into normalized grey scale (8-bit) to achieve maximum contrast. Also, the mean diameter and area of pores or interstices were determined through Image J software, according to Pugnaloni, Matia-Merino and Dickinson (Pugnaloni, Matia-Merino, & Dickinson, 2005). The effect of time of hydrolysis on both parameters was evaluated using a Mixed-Model Nested ANOVA Design ($p < 0.05$). A Tukey HSD test was performed to analyze the mean differences between the levels of the time factor of hydrolysis.

### *2.17. Statistical analysis*

The data are reported as the average values ± their standard deviations. Statistical analyses were performed with Sigma Plot v.10.0, Origin v.6.1 and Statgraph v.5.0 softwares. The relationship between variables was statistically analyzed by correlation analysis using Pearson correlation coefficient (p). The differences were considered statistically significant at $p < 0.05$ values.

## 3. Results and Discussion

### *3.1. NaCAS hydrolysis by P7PP*

P7PP displayed a proteolytic activity, as assayed by the azocasein method, of 70 U $mL^{-1}$ (1,600 U mg $protein^{-1}$). Hydrolysis of NaCAS with P7PP was carried out for up to 7 h and, during this period, the DH was determined in hydrolysate supernatants (Figure 1). Although the DH reached 8.2% after 7 h, higher hydrolysis rates were observed in the first four hours of hydrolysis, where the DH approached 6.2% in $t_4$, decreasing afterwards. Since the DH measures the number of cleaved peptide bonds, the slower rates of DH increase

indicate the lesser availability of cleavable peptide in the protein substrate, a behavior that is governed by enzyme specificity. A similar DH profile was observed for bovine NaCAS hydrolysates obtained with *Bacillus* sp. P45 protease (Hidalgo, et al., 2012). However, during ovine NaCAS hydrolysis with P7PP, the release of amino groups (or peptide bonds cleaved) was somewhat lower during the hydrolysis process, which might reflect substrate (caseins) heterogeinity across species (Minervini, et al., 2003).

**Figure 1**

According to the electrophoretic profiles, the molecular mass of all hydrolysates was below 6,000 Da. These hydrolysates did not remain in the electrophoretic gel (data not shown), even at high concentrations of polyacrylamide.

The results of peptide mass distribution confirmed that the highest proportion of molecular masses of the hydrolysates obtained until 4 h of hydrolysis were lower than 3,000 Da (Figure 2). However, a little portion of peptides with molecular masses between 3,000 and 5,000 Da during the first hydrolysis times measured was observed (data not shown).

**Figure 2**

Peptides with a signal/noise ratio higher than 10 were fragmented and their sequences were studied. Four peptides with a small size between 10 and 20 amino acid residues were identified. Molecular masses of 1140.67, 1641.90, 1788.96 and 2107.23 Da correspond to the sequences RPKHPIKHQG, QGLPQEVLNENLLRFF, QGLPQEVLNENLLRFFV and

346 FLLYQEPVLGPVRGPFPIIV, respectively. These peptides constitute fractions of $\alpha_{S1}$-CN
347 (f1-10), $\alpha_{S1}$-CN (f9-24), $\alpha_{S1}$-CN (f9-25) and β-CN (f190-209), respectively.

348 Among these peptides, two of them represented β-CN C-terminal and $\alpha_{S1}$-CN N-initial
349 fragments. On the other hand, in general, the P7PP cleavage occurred in the junction
350 between two residues with nonpolar side chains, such as F-V, V-A, G-L, A-F. Although
351 other authors have not reported the exact sequence of these peptides, different fragments of
352 these sequences have been informed. Larsen et al. (2010) have reported the existence of
353 peptides in the milk of cows previously infected with the mastitis virus, with similar
354 sequences to those we have identified: $\alpha_{S1}$-CN (f2-22), $\alpha_{S1}$-CN (f8-21), β-CN (f199-209),
355 β-CN (f192-209), β-CN (f193-209) (Larsen, et al., 2010). Also, Bezerra (2011) identified
356 three peptides employing a *Penicillium auratiogriseum* protease to hydrolyze caprine milk.
357 These β-CN peptides presented similar sequences compared with those we obtained: β-CN
358 (f191-207), β-CN (f194-202) and β-CN (f191-206). These authors reported that these β-CN
359 fragments showed antioxidant activities in vitro (Bezerra, 2011). On the other hand,
360 Andriamihaja et al. (2013) employed two microbial enzymatic preparations from *Bacillus*
361 *subtilis* and pancreatin with the aim of generating small, medium-size and large
362 polypeptides from bovine CN during 2 h of hydrolysis. They have reported the presence of
363 two peptides from β-CN and five from $\alpha_{S1}$-CN, whose sequences, in some fragments, were
364 consistent with those identified in our work: β-CN (f191-209), β-CN (f191-207), $\alpha_{S1}$-CN
365 (f1-13), $\alpha_{S1}$-CN (f1-16), $\alpha_{S1}$-CN (f1-15), $\alpha_{S1}$-CN (f1-19), $\alpha_{S1}$-CN (f1-20) (Andriamihaja, et
366 al., 2013). Finally, Kalyankar et al. (2013) reported the presence of three peptides from $\alpha_{S1}$-
367 CN (f1-18, f1-30, f3-30) using a glutamyl endopeptidase from Alcalase™ during 2 h of
368 hydrolysis (Kalyankar, Zhu, O' Keeffe, O' Cuinn, & FitzGerald, 2013).

*3.2. Intrinsic fluorescence spectra and surface hydrophobicity*

Emission spectra of NaCAS and the hydrolysates obtained at different times of hydrolysis ($t_i$) are presented in Figure 3.

**Figure 3**

Hydrolysis caused a fluorescence red shift as well as a decrease in the fluorescence intensity (FI), which might be due to conformational changes. These changes would indicate an increment of the polarity in the surroundings of intrinsic fluorophore groups in the peptides (Trp and Tyr). Previously, it was verified that during enzymatic proteolysis there was no loss of protein fluorophores occurs (data not shown).

$S_0$ ($g/100g^{-1}$) of NaCAS hydrolysates decreased as $t_i$ increased (except for $t_1$): $t_0$=111.2±0.2, $t_1$=170.1±0.2, $t_2$=83.4±0.2, $t_3$ =31.4±0.3. In the case of hydrolysate $t_4$, $S_0$ determination could not be carried out. These results would indicate that after 1 h of hydrolysis, a higher exposure of hydrophobic groups occurs on the protein surface. However, the decrease of $S_0$ as $t_i$ increased would indicate that there is a reduction in the amount of hydrophobic residues of peptides in hydrolysates.

*3.3. Evaluation of hydrolysates bioactivities in vitro*

*3.3.1. Antioxidant activity*

Peptides and protein hydrolysates, obtained from the proteolysis of various food proteins, are reported to possess antioxidant activities. Antioxidant activities might protect

biological systems against damage related to oxidative stress in human disease conditions. These antioxidant peptides and hydrolysates might also be employed in preventing oxidation reactions (such as lipid peroxidation) that lead to deterioration of foods and foodstuffs (Hogan, Zhang, Li, Wang, & Zhou, 2009; L. Zhang, J. Li, & K. Zhou, 2010). The antioxidant activities, including ABTS radical scavenging, reducing power and ferrous ion chelating ability of the hydrolysates were evaluated.

**Table 1**

The radical $ABTS^{\bullet+}$ scavenging ability of hydrolysates increased, reaching a maximum at $t_6$ (Table 1). Although NaCAS also exhibits antioxidant activity, the increment of this activity as the hydrolysis time increases suggests that the proteolytic process contributes to the biological activity.

Megías et al. reported that histidine may be considered as a strong metal chelator due to the presence of an imidazole ring (Megías, et al., 2008). According to the results, it would seem that hydrolysis increases the accessibility of the metal to the casein histidine groups. Therefore, these results indicate that the hydrolysis of NaCAS could be useful to increase mineral bioavailability. Also, NaCAS hydrolysates could be used as natural antioxidants to prevent oxidation reactions in the development of functional food products and additives.

Transition metals such as $Fe^{2+}$ promote the lipid peroxidation and then their chelation helps to retard the peroxidation and prevent food rancidity (Lei Zhang, Jianrong Li, & Kequan Zhou, 2010). As observed in Table 2, NaCAS without hydrolysis presents iron

chelation activity (78.400 ± 0.005%). This activity was significantly increased when the hydrolysis occur, reaching a maximum of 94.60 ± 0.04 % at $t_3$.

The reducing power assay is based on the capability of hydrolysates to reduce the $Fe^{3+}$/ferricyanide complex to the ferrous form. The results showed in Table 2 suggest that NaCAS hydrolysates would act as electron donors reducing the oxidized intermediates of lipidic peroxidation. The fact that the reducing power of the NaCAS hydrolysates is associated with this antioxidant activity suggested that the reducing power was likely to contribute significantly towards the observed antioxidant effect (Corrêa, et al., 2011; Zhu, et al., 2006). The reducing power of the hydrolysates reached a maximum value at $t_3$ and then diminished. According to mass spectrometry assays, the amount of small peptides increases as hydrolysis time increases. This suggests that the higher molecular mass of the hydrolysate, the higher reducing power activity. This behavior was also reported by other authors (Corrêa, et al., 2011; Chang, et al., 2007).

*3.3.2. Antibacterial activity*

The ability of NaCAS hydrolysates to inhibit the growth of many bacteria was then investigated. The results obtained are shown in Table 2.

**Table 2**

Both Gram-positive and Gram-negative bacteria were inhibited but only the $t_{0.5}$ and $t_1$ hydrolysates inhibited the growth of *Salmonella Enteritidis*, *Escherichia coli*, *Corynebacterium fimi* and *Listeria monocytogenes*. These results are important because of these inhibited bacteria are important microorganisms related to foodborne diseases (Mor-

Mur & Yuste, 2010). The antimicrobial activity observed for the NaCAS hydrolysates by the action of P7PP might represent a promising application to prevent the contamination of foods by these pathogenic microorganisms. Further interest is focused on caseins since these are safe food proteins abundantly available at low costs. Other authors have reported the identification of antibacterial domains within the sequence of bovine $\alpha_{S2}$-CN (McCann, et al., 2005; Recio & Visser, 1999), of $\alpha_{S1}$-CN (McCann, et al., 2006; Wu, et al., 2013), of β-CN (Wu, et al., 2013) and of κ-CN (Arruda, et al., 2012). Particularly, Arruda et al. (2012) obtained fragments of $\alpha_{S1}$-CN (f1-21, f1-23 and f8-23) and β-CN (f189-203) by casein hydrolysis during 2 h employing a new protease obtained from latex *Jacaratia corumbensis*. The sequence of these fragments, which partially coincides with $\alpha_{S1}$-CN (f1-10, f9-24 and f9-25) and β-CN (f190-209) fragments previously reported in this work, demonstrate antibacterial activity against *Enterococcus faecalis*, *Bacillus subtilis*, *Escherichia coli*, *Pseudomonas aeruginosa*, *Klebsiella pneumonia* and *Staphylococcus aureus* (Arruda, et al., 2012).

The higher susceptibility of Gram-positive microorganisms to casein-derived peptides, when compared to Gram-negative bacteria, might be attributed to the more complex cellular envelope of the latter (López-Expósito, Gómez-Ruiz, Amigo, & Recio, 2006).

*3.4. Acid aggregation of NaCAS hydrolysates*

The acid aggregation of NaCAS hydrolysates was evaluated by the variations of $A_{650nm}$ as a function of time (Figure 4A). The results show that the hydrolysates did not maintain the capability to aggregate, except for $t_0$, which is the sample that was not hydrolyzed

(control). The absence of formation of aggregates from $t_{1-7}$ hydrolysates, detectable by this technique, is probably due to the small average size of the particles that do not form aggregates or generate a small aggregates (smaller than the incident $\lambda$) not detected by turbidity measurements.

**Figure 4**

On the other hand, no changes on the rate at which pH becomes lower were detected (Figure 4B).

*3.5. Acid aggregation of NaCAS:hydrolysates mixtures*

With the aim of evaluating whether the addition of the hydrolysates with biological activities modifies the kinetics of NaCAS aggregation and / or the degree of compactness of the aggregate formed, acid aggregation of NaCAS:hydrolysates mixtures (4:1) was evaluated analyzing how parameter $\beta$ is modified as a function of time and pH after adding GDL (Figure 5).

**Figure 5**

The aggregation process observed was similar to those previously reported for non-hydrolyzed bovine NaCAS and reveals two well-defined steps (Hidalgo, et al., 2011). At the first aggregation stage, the decrease in the average diameters, estimated by $\beta$ values, may be due to a dissociation of pre-existing aggregates along together with the formation of

a large amount of new aggregates of smaller size due to a loss of the net charge of the particles, which reduces their electrostatic stability and makes them more susceptible to flocculation. At pH values near the isoelectric point, the higher number of particles with electrostatic destabilization causes the formation of much larger particle size aggregates.

In presence of hydrolysates, changes in the time at which the second step starts ($t_{ag}$) were observed (increment of $t_{ag}$) but the pH value observed at $t_{ag}$ ($pH_{ag}$) was shown to be similar to that of non-hydrolysed NaCAS. There were also no changes on the rate at which the pH becomes lower. These results indicate that the electrostatic stability of NaCAS is not appreciably affected by the presence of hydrolysates.

On the other hand, the decrease of superficial hydrophobic residues as hydrolysis time increases (estimated by $S_0$ values), the probability of hydrophobic interactions between destabilized particles diminishes. Therefore, as hydrolysis time increases, the time at which the aggregates formation starts is higher.

As from the estimation of the fractal dimension by turbidimetry, no significant changes were observed in the degree of compactness of the aggregates ($D_f$) formed at the end of the acidification process of NaCAS:hydrolysate mixtures at low concentrations (Table 3).

**Table 3**

Taking into account these results, it is important to assess the behavior of these mixtures at concentrations at which the decrease in pH leads to the formation of acid gels. Therefore, the rheological behavior and the microstructure of such gels were evaluated.

*3.6. Rheological behavior of NaCAS:hydrolysate mixtures*

Aiming at studying the effect of the presence of the hydrolysates on NaCAS gelation, the acid gelation process of NaCAS:hydrolysate mixtures was studied. Previously, it was found that the hydrolysates did not form acid gels after adding GDL. From the G′ and G″ vs. time plots, the gel point was determined as the time when the G′ and G″ crossover ($t_g$) occurred (Curcio, et al., 2001). pH at $t_g$ was also determined considering the pH value at the G′ and G″ crossover ($pH_g$). Both $t_g$ and $pH_g$ showed no significant changes at all $t_i$ assayed (i=0-4) (data not shown). After gel point, G′ and G″ increased up to a steady-state, G′ being higher than G″ in all cases. Figure 6 shows the variation of the complex shear modulus (G*) vs. acidification time. Differences among the gels produced in the presence of hydrolysates at the beginning of the gelation process can be observed.

**Figure 6**

The non-linear least-square regression method was used to fit the raw mechanical properties data as a function of acidification time:

$$G^* = G^*_{eq} + C\, e^{-k t} \quad (2)$$

where $G^*_{eq}$ is the steady-state G* value, k is the initial rate of increase in G*, t is the time after GDL addition and C is a fitting parameter (Cavallieri & da Cunha, 2008). The values of $G^*_{eq}$ and k are shown in Table 4.

**Table 4**

At the beginning of gelation, the increase in G* could reflect the increased contact between the NaCAS particles mediated by particle fusion, and subsequent interparticle rearrangements due to bond reversibility, which result in more bonds per junction and in more junctions, which in turn increases the storage modulus (Mellema, Walstra, van Opheusden, & van Vliet, 2002). According to our results, $G^*_{eq}$ and k diminish in the presence of hydrolysates obtained at higher $t_i$, especially for hydrolysate $t_4$. Therefore, the presence of hydrolysates would make the interparticle rearrangements difficult leading to a decrease of elastic character of gels.

*3.7. Evaluation of gel microstructure*

Figure 7 shows representative microscopic images of NaCAS:hydrolysate $t_0$ and NaCAS:hydrolysate $t_4$ gels which were captured using CLSM. These images provide visual information regarding how the presence of hydrolysates affects the microstructure of NaCAS gels. Red pixels in the images are due to polypeptide chains dyed with Rhodamine B, while the black pixels are due to interstices formed. The CLSM images show a porous stranded network structure.

**Figure 7**

A comparison of both images indicates that the NaCAS gel network depends on the presence of hydrolysates. The pores around the polypeptide network become smaller with the increase in $t_i$ (Table 5). Also, the pore diameter distribution indicates that the amount of

552 smaller interstices was the highest for NaCAS:hydrolysate $t_4$ gels (Figure 8). Therefore, as $t_i$
553 increases, the amount of pores increases and these pores are even smaller.
554
555 **Table 5**
556 **Figure 8**
557
558 On the other hand, from the analysis of textural parameters (Table 6), we could
559 conclude that the presence of hydrolysates ($t_{1-4}$) increases S and decreases U values.
560 According to U values, $t_0$ image is smoother (more uniform) than $t_4$ image; i.e.,
561 microstructure for NaCAS:hydrolysate $t_4$ gel is more disordered. S values lead us to the
562 same conclusion; $t_0$ image has the lowest variation in grey level. Therefore, the presence of
563 hydrolysates ($t_{1-4}$) would make the ordered structure of NaCAS gels weaker. This
564 observation is consistent with the lower value of G* of these mixed gels (Figure 6).
565
566 **Table 6**
567
568 **4. Conclusions**
569 This study shows that a protease preparation from *Bacillus* sp. P7 could be used in the
570 hydrolysis of bovine NaCAS to obtain peptides possessing different antioxidant and
571 antimicrobial activities. Some of these peptides are fractions of $\alpha_{S1}$-CN and β-CN, and
572 parts of their sequences, with antioxidant and antibacterial activities, have been previously
573 reported. The isolation of such bioactive peptides will be studied in further work.

The hydrolysates did not maintain the capability to aggregate under acid conditions when GDL was added. However, their incorporation in NaCAS solutions modifies the kinetics of the acid aggregation process but does not significantly alter the degree of compactness of the aggregate formed at low NaCAS concentration. On the other hand, at NaCAS concentrations where the decrease in pH leads to the formation of acid gels, the presence of hydrolysates leads to more porous and weaker gels, especially in the presence of hydrolysate $t_4$. Therefore, these results suggest that these bioactive peptides modify the microstructure and rheological behavior when they are added into NaCAS acid gels.

**Acknowledgements**

This work was supported by grants from the Universidad Nacional de Rosario, Agencia Nacional de Promoción Científica y Tecnológica (PICT 2011 1354), the Cooperation Program between Coordenação de Aperfeiçoamento de Pessoal de Nível Superior (CAPES) from Brazil and the Ministerio de Ciencia, Tecnología e Innovación Productiva (MINCyT) from Argentine). Thanks to María Robson, Mariana de Sanctis and Geraldine Raimundo, for the English revision, to Bibiana Riquelme for image analysis, to Hebe Bottai for statistical analysis and to Silvia Moreno, Maria Pía Valacco and Ricardo Neme Tauil, from the CEQUIBIEM, for the mass spectrometry service.

**Figure captions**

**Fig.1:** Degree of hydrolysis (DH) of NaCAS obtained with a protease preparation from *Bacillus* sp. P7 (P7PP).

**Fig. 2:** Peptide mass distribution determined by MALDI-TOF-TOF mass spectrometry of hydrolysates obtained from NaCAS hydrolysis with P7PP for 1 ($t_1$), 2 ($t_2$), 3 ($t_3$) and 4 ($t_4$) hours.

**Fig. 3:** Fluorescence emission spectra of the hydrolysates obtained through proteolysis with P7PP at different times ($t_i$): (●) NaCAS without hydrolysis; (○) $t_0$; (▲) $t_1$; (Δ) $t_2$; (■) $t_3$; (□) $t_4$; (◊) $t_7$, where the subscript i correspond to the hydrolysis time. Hydrolysates concentration = 1 mg $g^{-1}$; Range of $\lambda_{em}$ = 300-420nm, $\lambda_{exc}$ 286nm; T 35ºC.

**Fig. 4:** Variations of the absorbance at 650 nm ($A_{650nm}$) (A) and pH (B) as a function of time, after glucono-δ-lactone (GDL) addition, during the acid aggregation of NaCAS hydrolysates $t_0$ (●), $t_1$ (Δ), $t_2$ (▲), $t_3$ (□), $t_4$ (■), and $t_7$ (◊),where the subscript i correspond to the hydrolysis time. Assays performed at 35ºC; GDL mass fraction/protein mass fraction (R) = 0.5; hydrolysates concentration = 5 mg $g^{-1}$.

**Fig. 5:** Variations of parameter β, proportional to the average size of particles, as a function of time (A) and pH (B), after glucono-δ-lactone (GDL) addition, during the acid aggregation of NaCAS:hydrolysates mixtures (4:1): NaCAS without hydrolysate (○), with $t_0$ (●), with $t_1$ (Δ), with $t_2$ (▲), with $t_3$ (□), with $t_4$ (■), and with $t_7$ (◊), where the subscript i correspond to the hydrolysis time. Assays performed at 35ºC; GDL mass fraction/protein mass fraction (R) = 0.5; NaCAS:hydrolysates total concentration = 5 mg $g^{-1}$

**Fig. 6:** Time dependence of the complex modulus G* (at 0.1 Hz) for NaCAS:hydrolysates mixtures (4:1) acid gels obtained at different hydrolysis times ($t_i$): NaCAS:hydrolysate $t_i$: $t_0$ (●), $t_1$ (Δ),$t_2$ (▲), $t_3$ (□), $t_4$ (■), where the subscript i correspond to the hydrolysis time.

NaCAS concentration: 30 mg $g^{-1}$, hydrolysate concentration: 7.5 mg $g^{-1}$, R = 0.5 and T = 35 ºC.

**Fig. 7:** Microphotographs of NaCAS:hydrolysates $t_0$ and $t_4$ gels obtained by CLSM, using Rhodamine B (2 x $10^{-3}$ mg $mL^{-1}$). NaCAS concentration: 30 mg $g^{-1}$, hydrolysate concentration: 7.5 mg $g^{-1}$, R = 0.5 and T = 35 ºC.

**Fig. 8:** Pore diameter distribution of NaCAS:hydrolysates gels obtained by addition of GDL at 35°C. NaCAS concentration: 30 mg $g^{-1}$, hydrolysate concentration: 7.5 mg $g^{-1}$, R = 0.5.

## References


Adler-Nissen, J. (1979). Determination of the degree of hydrolysis of food protein hydrolysates by trinitrobenzenesulfonic acid. *Journal of Agricultural and Food Chemistry, 27*(6), 1256-1262.

Alvarez, E., Risso, P., Gatti, C., Burgos, M., & Suarez Sala, V. (2007). Calcium-induced aggregation of bovine caseins: effect of phosphate and citrate. *Colloid & Polymer Science, 285*(5), 507-514.

Andriamihaja, M., Guillot, A., Svendsen, A., Hagedorn, J., Rakotondratohanina, S., Tomé, D., & Blachier, F. (2013). Comparative efficiency of microbial enzyme preparations versus pancreatin for in vitro alimentary protein digestion. *Amino Acids, 44*(2), 563-572.

Arruda, M. S., Silva, F. O., Egito, A. S., Silva, T. M. S., Lima-Filho, J. L., Porto, A. L. F., & Moreira, K. A. (2012). New peptides obtained by hydrolysis of caseins from bovine milk by protease extracted from the latex Jacaratia corumbensis. *LWT - Food Science and Technology, 49*(1), 73-79.

Bezerra, V. S. (2011). *Caracterização e atividade biológica de peptídeos obtidos pela hidrólise enzimática de caseína do leite de cabra Moxotó (Capra hircus Linnaeus, 1758).* Unpublished Doutorado em Biociência Animal, Universidade Federal Rural de Pernambuco, Recife.

Braga, A. L. M., Menossi, M., & Cunha, R. L. (2006). The effect of the glucono-[delta]-lactone/caseinate ratio on sodium caseinate gelation. *International Dairy Journal, 16*(5), 389-398.

Camerini-Otero, R. D., & Day, L. A. (1978). The wavelength dependence of the turbidity of solutions of macromolecules. *Biopolymers, 17*(9), 2241-2249.

Cavallieri, A. L. F., & da Cunha, R. L. (2008). The effects of acidification rate, pH and ageing time on the acidic cold set gelation of whey proteins. *Food Hydrocolloids, 22*(3), 439-448.

Corrêa, A. P. F., Daroit, D. J., & Brandelli, A. (2010). Characterization of a keratinase produced by Bacillus sp. P7 isolated from an Amazonian environment. *International Biodeterioration & Biodegradation, 64*(1), 1-6.

Corrêa, A. P. F., Daroit, D. J., Coelho, J., Meira, S. M. M., Lopes, F. C., Segalin, J., Risso, P. H., & Brandelli, A. (2011). Antioxidant, antihypertensive and antimicrobial properties of ovine milk caseinate hydrolyzed with a microbial protease. *Journal of the Science of Food and Agriculture, 91*(12), 2247-2254.

Corzo-Martínez, M., Moreno, F. J., Villamiel, M., & Harte, F. M. (2010). Characterization and improvement of rheological properties of sodium caseinate glycated with galactose, lactose and dextran. *Food Hydrocolloids, 24*(1), 88-97.

Curcio, S., Gabriele, D., Giordano, V., Calabrò, V., de Cindio, B., & Iorio, G. (2001). A rheological approach to the study of concentrated milk clotting. *Rheologica Acta, 40*(2), 154-161.

Chang, C.-Y., Wu, K.-C., & Chiang, S.-H. (2007). Antioxidant properties and protein compositions of porcine haemoglobin hydrolysates. *Food Chemistry, 100*(4), 1537-1543.

de Kruif, C. G. (1997). Skim Milk Acidification. *Journal of Colloid and Interface Science, 185*(1), 19-25.

FitzGerald, R. J., Murray, B. A., & Walsh, D. J. (2004). Hypotensive peptides from milk proteins. *Journal of Nutrition, 134*(4), 980S-988S.

Gonzalez, J., & Woods, R. E. (2001). *Digital Image Processing* (Second ed.): Prentice Hall.

Gupta, R., Beg, Q. K., & Lorenz, P. (2002). Bacterial alkaline proteases: molecular approaches and industrial applications. *Applied Microbiology and Biotechnology, 59*(1), 15-32.

Haque, E., & Chand, R. (2008). Antihypertensive and antimicrobial bioactive peptides from milk proteins. *European Food Research and Technology, 227*(1), 7-15.

Hartmann, R., & Meisel, H. (2007). Food-derived peptides with biological activity: from research to food applications. *Current Opinion in Biotechnology, 18*(2), 163-169.

Hidalgo, M. E., Daroit, D. J., Folmer Corrêa, A. P., Pieniz, S., Brandelli, A., & Risso, P. H. (2012). Physicochemical and antioxidant properties of bovine caseinate hydrolysates obtained through microbial protease treatment. *International Journal of Dairy Technology, 65*(3), 342-352.

Hidalgo, M. E., Mancilla Canales, M. A., Nespolo, C. R., Reggiardo, A. D., Alvarez, E. M., Wagner, J. R., & Risso, P. H. (2011). Comparative study of bovine and ovine caseinate aggregation processes: Calcium-induced aggregation and acid aggregation. In D. A. Stein (Ed.), *Protein Aggregation* (pp. 199-222). Hauppauge, NY: Nova Publishers.

Hogan, S., Zhang, L., Li, J., Wang, H., & Zhou, K. (2009). Development of antioxidant rich peptides from milk protein by microbial proteases and analysis of their effects on lipid peroxidation in cooked beef. *Food Chem., 117*, 438–443.

Horne, D. S. (1987). Determination of the fractal dimension using turbidimetric techniques. Application to aggregating protein systems. *Faraday Discussions of the Chemical Society, 83*(0), 259–270.

Kalyankar, P., Zhu, Y., O' Keeffe, M., O' Cuinn, G., & FitzGerald, R. J. (2013). Substrate specificity of glutamyl endopeptidase (GE): Hydrolysis studies with a bovine α-casein preparation. *Food Chemistry, 136*(2), 501-512.

Kato, A., & Nakai, S. (1980). Hydrophobicity determined by a fluorescence probe method and its correlation with surface properties of proteins. *Biochimica et Biophysica Acta (BBA) - Protein Structure, 624*(1), 13-20.

Korhonen, H. (2009). Milk-derived bioactive peptides: from science to applications. *J. Funct. Foods, 1*, 177-187.

Kuaye, A. Y. (1994). An ultraviolet spectrophotometric method to determine milk protein content in alkaline medium. *Food Chemistry, 49*(2), 207-211.

Laemmli, U. K. (1970). Cleavage of structural proteins during the assembly of the head of bacteriophage T4. *Nature, 227*, 680-685.

Larsen, L. B., Hinz, K., Jørgensen, A. L. W., Møller, H. S., Wellnitz, O., Bruckmaier, R. M., & Kelly, A. L. (2010). Proteomic and peptidomic study of proteolysis in quarter milk after infusion with lipoteichoic acid from Staphylococcus aureus. *Journal of Dairy Science, 93*(12), 5613-5626.

Li, B., Chen, F., Wang, X., Ji, B., & Wu, Y. (2007). Isolation and identification of antioxidative peptides from porcine collagen hydrolysate by consecutive chromatography and electrospray ionization-mass spectrometry. *Food Chemistry, 102*(4), 1135-1143.

López-Expósito, I., Gómez-Ruiz, J., Amigo, L., & Recio, I. (2006). Identification of antibacterial peptides from ovine α s2-casein. *Int. Dairy J. , 16*, 1072-1080.

Mancilla Canales, M. A., Hidalgo, M. E., Risso, P. H., & Alvarez, E. M. (2010). Colloidal Stability of Bovine Calcium Caseinate Suspensions. Effect of Protein Concentration and the Presence of Sucrose and Lactose. *Journal of Chemical & Engineering Data, 55*(7), 2550-2557.

McCann, K. B., Shiell, B. J., Michalski, W. P., Lee, A., Wan, J., Roginski, H., & Coventry, M. J. (2005). Isolation and characterisation of antibacterial peptides derived from the f(164–207) region of bovine αS2-casein. *International Dairy Journal, 15*(2), 133-143.

McCann, K. B., Shiell, B. J., Michalski, W. P., Lee, A., Wan, J., Roginski, H., & Coventry, M. J. (2006). Isolation and characterisation of a novel antibacterial peptide from bovine αS1-casein. *International Dairy Journal, 16*(4), 316-323.

Megías, C., Pedroche, J., Yust, M. M., Girón-Calle, J., Alaiz, M., Millán, F., & Vioque, J. (2008). Production of copper-chelating peptides after hydrolysis of sunflower proteins with pepsin and pancreatin. *LWT - Food Science and Technology, 41*(10), 1973-1977.

Mellema, M., Walstra, P., van Opheusden, J. H., & van Vliet, T. (2002). Effects of structural rearrangements on the rheology of rennet-induced casein particle gels. *Advances in Colloid and Interface Science, 98*(1), 25-50.

Minervini, F., Algaron, F., Rizzello, C. G., Fox, P. F., Monnet, V., & Gobbetti, M. (2003). Angiotensin I-Converting-Enzyme-Inhibitory and Antibacterial Peptides from Lactobacillus helveticus PR4 Proteinase-Hydrolyzed Caseins of Milk from Six Species. *Applied and Environmental Microbiology, 69*(9), 5297-5305.

Mor-Mur, M., & Yuste, J. (2010). Emerging bacterial pathogens in meat and poultry: an overview. *Food Bioprocess Technol. , 3*, 24-35.

Motta, A., & Brandelli, A. (2002). Characterization of an antibacterial peptide produced by Brevibacterium linens. *Journal of Applied Microbiology, 92*(1), 63-70.

Mulvihill, D. M., & Fox, P. F. (1989). Caseins and manufactured. In P. F. F. Ed. (Ed.), *Development in Dairy Chemistry* (Vol. 4, pp. 97-130). London & New York: Elsevier Applied Science.

Nishinari, K., Zhang, H., & Ikeda, S. (2000). Hydrocolloid gels of polysaccharides and proteins. *Current Opinion in Colloid & Interface Science, 5*(3-4), 195-201.

Phelan, M., Aherne, A., FitzGerald, R. J., & O'Brien, N. M. (2009). Casein-derived bioactive peptides: Biological effects, industrial uses, safety aspects and regulatory status. *International Dairy Journal, 19*(11), 643-654.

Pugnaloni, L. A., Matia-Merino, L., & Dickinson, E. (2005). Microstructure of acid-induced caseinate gels containing sucrose: Quantification from confocal microscopy and image analysis. *Colloids and Surfaces B: Biointerfaces, 42*(3-4), 211-217.

Rabiey, L., & Britten, M. (2009). Effect of whey protein enzymatic hydrolysis on the rheological properties of acid-induced gels. *Food Hydrocolloids, 23*(8), 2302-2308.

Rao, M. B., Tanksale, A. M., Ghatge, M. S., & Deshpande, V. V. (1998). Molecular and Biotechnological Aspects of Microbial Proteases. *Microbiology and Molecular Biology Reviews, 62*(3), 597-635.

Re, R., Pellegrini, N., Proteggente, A., Pannala, A., Yang, M., & Rice-Evans, C. (1999). Antioxidant activity applying an improved ABTS radical cation decolorization assay. *Free Radic BiolMed 26*, 1231–1237.

Recio, I., & Visser, S. (1999). Identification of two distinct antibacterial domains within the sequence of bovine αs2-casein. *Biochimica et Biophysica Acta (BBA) - General Subjects, 1428*(2–3), 314-326.

Risso, P., Relling, V., Armesto, M., Pires, M., & Gatti, C. (2007). Effect of size, proteic composition, and heat treatment on the colloidal stability of proteolyzed bovine casein micelles. *Colloid & Polymer Science, 285*(7), 809-817.

Rival, S. G., Boeriu, C. G., & Wichers, H. J. (2001). Caseins and casein hydrolysates. 2. Antioxidative properties and relevance to lipoxygenase inhibition. *J. Agric. Food Chem., 49*, 295–302.

Saiga, A., Tanabe, S., & Nishimiura, T. (2003). Antioxidant activity of peptides obtained from porcinemyofibrillar proteins by protease treatment. *J. Agric. Food Chem., 51*, 3661-3667.

Sarmadi, B. H., & Ismail, A. (2010). Antioxidative peptides from food proteins: A review. *Peptides, 31*(10), 1949-1956.

Silva, S. V., & Malcata, F. X. (2005). Caseins as source of bioactive peptides. *International Dairy Journal, 15*(1), 1-15.

Walstra, P., Jenness, R., & Badings, H. T. (1984). *Dairy chemistry and physics*. New York, USA: John Wiley & Sons.

Wu, S., Qi, W., Li, T., Lu, D., Su, R., & He, Z. (2013). Simultaneous production of multi-functional peptides by pancreatic hydrolysis of bovine casein in an enzymatic membrane reactor via combinational chromatography. *Food Chemistry, 141*(3), 2944-2951.

Zhang, L., Li, J., & Zhou, K. (2010). Chelating and radical scavenging activities of soy protein hydrolysates prepared from microbial proteases and their effect on meat lipid peroxidation. *Bioresource Technology, 101*(7), 2084-2089.

Zhang, L., Li, J., & Zhou, K. (2010). Chelating and radical scavenging activities of soy protein hydrolysates prepared from microbial proteases and their effect on meat lipid peroxidation. . *Bioresour. Technol., 101*, 2084–2089.

Zhu, K., Zhou, H., & Qian, H. (2006). Antioxidant and free radical-scavenging activities of wheat germ protein hydrolysates (WGPH) prepared with alcalase. *Process Biochemistry, 41*(6), 1296-1302.

**Graphical Abstract**

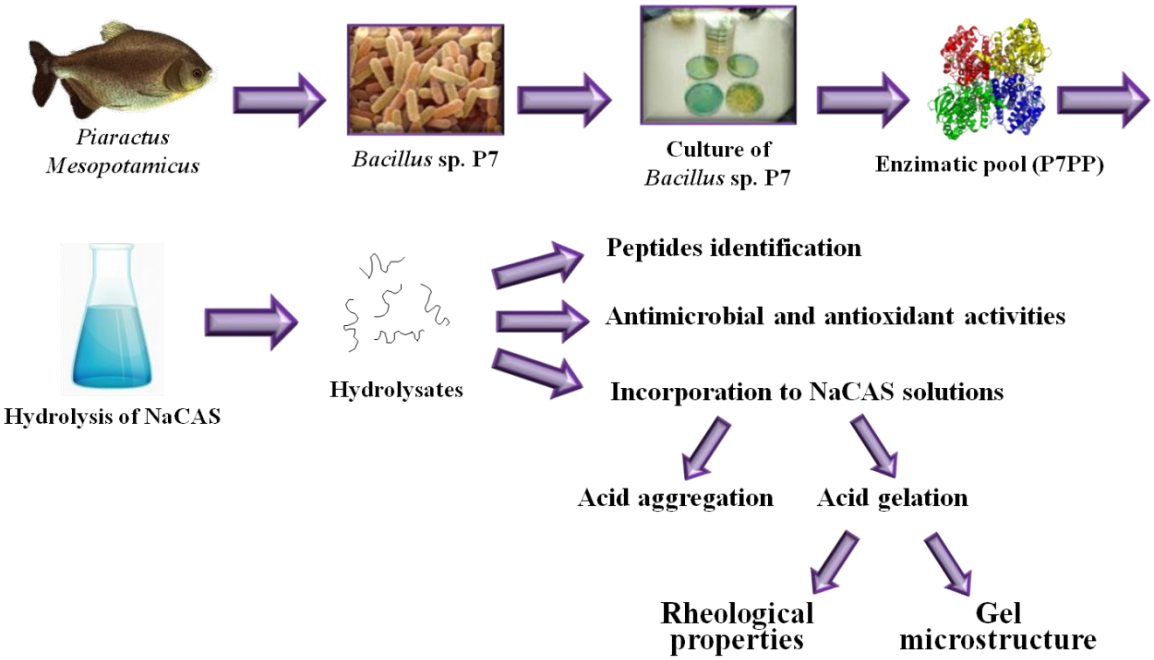

**Figure 1**

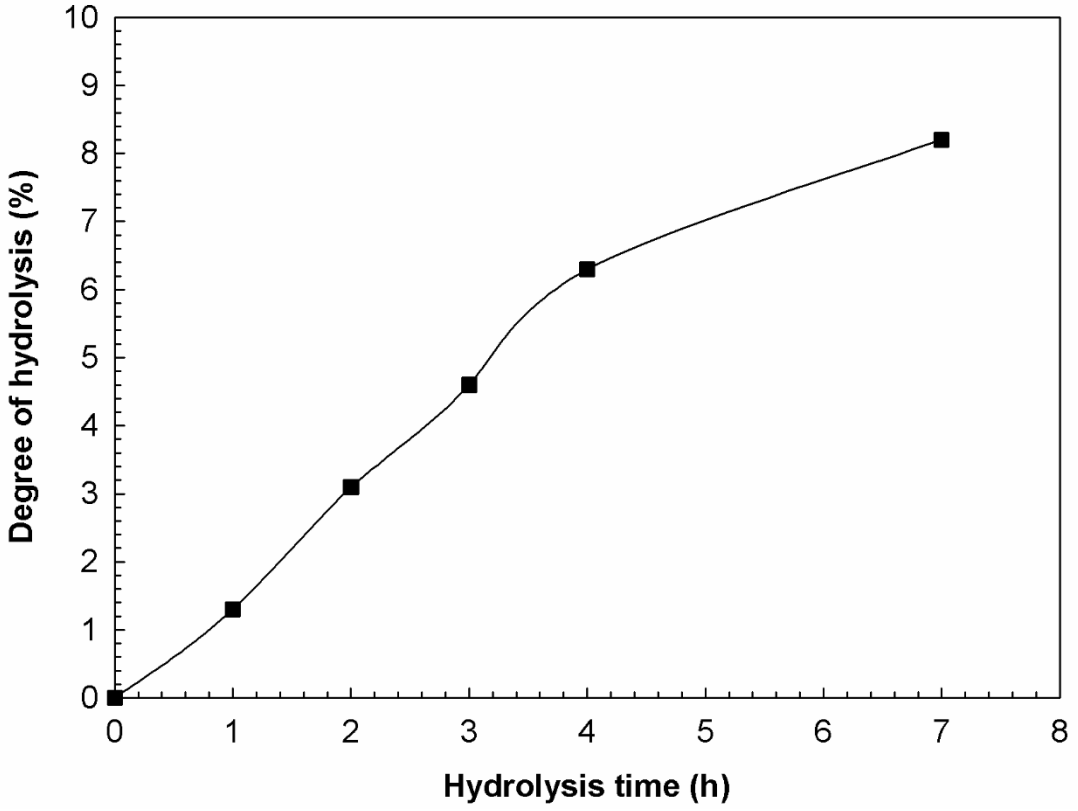


**Fig.1:** Degree of hydrolysis (DH) of NaCAS obtained with a protease preparation from *Bacillus* sp. P7 (P7PP).

**Figure 2**

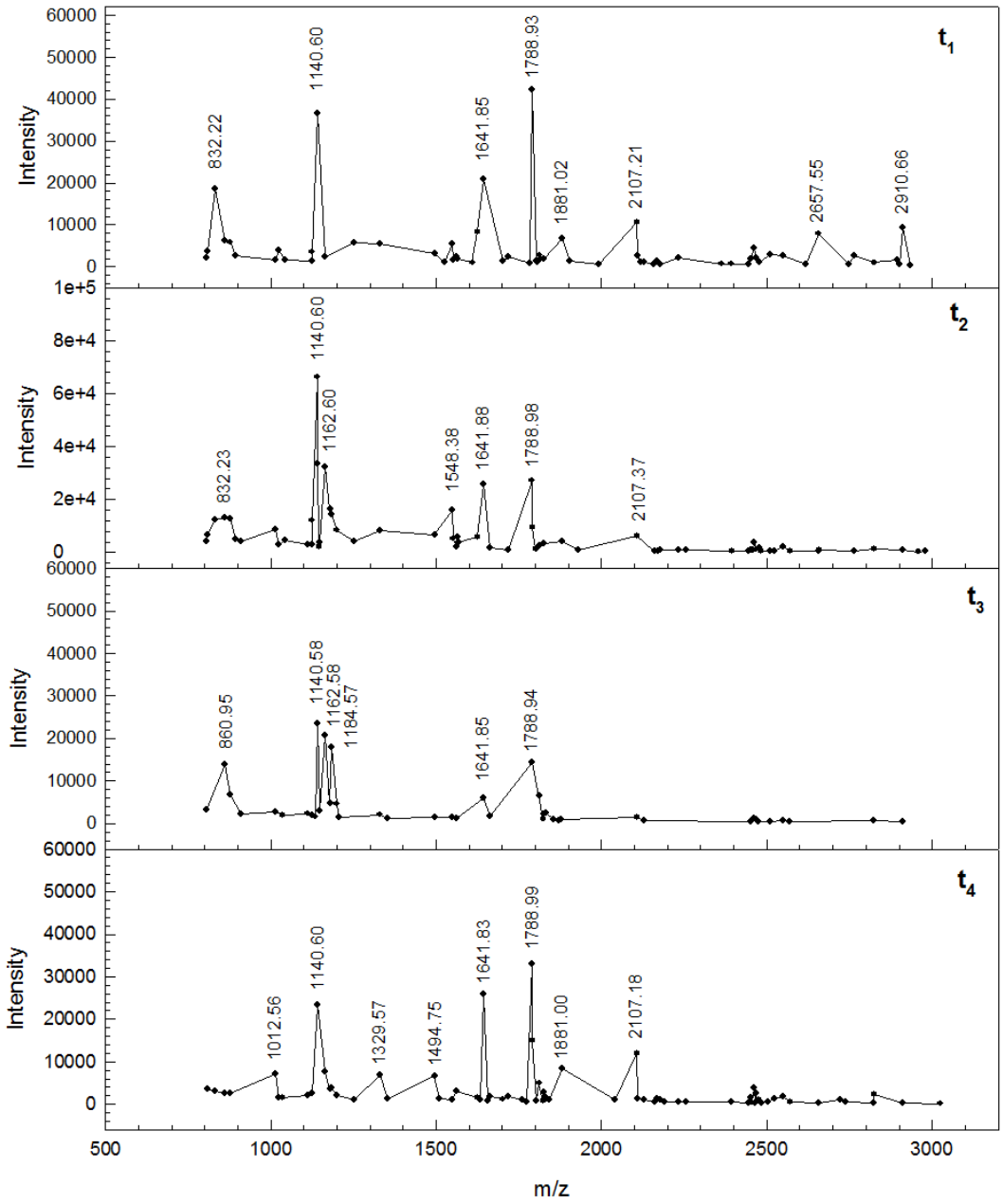


**Fig. 2:** Peptide mass distribution determined by MALDI-TOF-TOF mass spectrometry of hydrolysates obtained from NaCAS hydrolysis with P7PP for 1 ($t_1$), 2 ($t_2$), 3 ($t_3$) and 4 ($t_4$) hours.

**Figure 3**

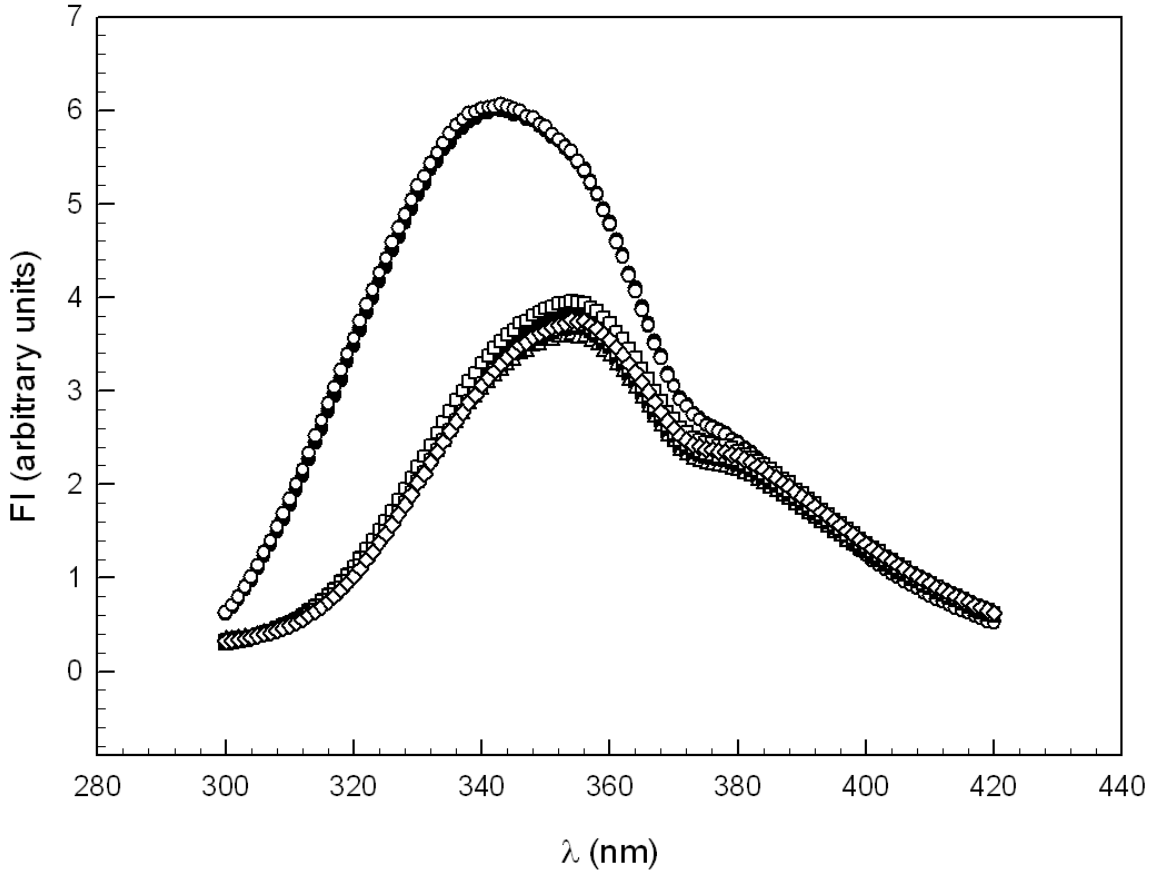


**Fig. 3:** Fluorescence emission spectra of the hydrolysates obtained through proteolysis with P7PP at different times ($t_i$): (●) NaCAS without hydrolysis; (○) $t_0$; (▲) $t_1$; (Δ) $t_2$; (■) $t_3$; (□) $t_4$; (◊) $t_7$, where the subscript i correspond to the hydrolysis time. Hydrolysates concentration = 1 mg $g^{-1}$; Range of $\lambda_{em}$ = 300-420nm, $\lambda_{exc}$ 286nm; T 35ºC.

**Figure 4**

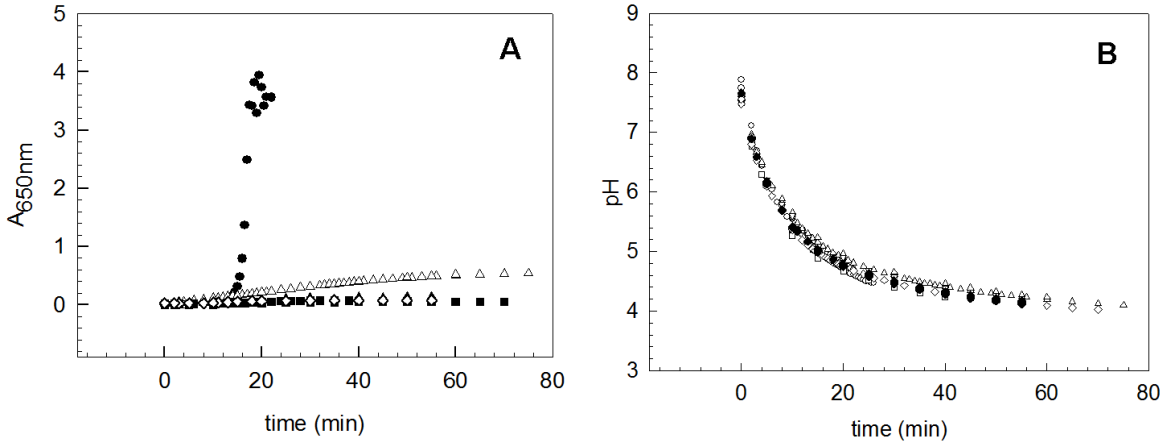


**Fig. 4:** Variations of the absorbance at 650 nm ($A_{650nm}$) (A) and pH (B) as a function of time, after glucono-δ-lactone (GDL) addition, during the acid aggregation of NaCAS hydrolysates $t_0$ (●), $t_1$ (Δ), $t_2$ (▲), $t_3$ (□), $t_4$ (■), and $t_7$ (◊),where the subscript i correspond to the hydrolysis time. Assays performed at 35ºC; GDL mass fraction/protein mass fraction (R) = 0.5; hydrolysates concentration = 5 mg $g^{-1}$.

**Figure 5**

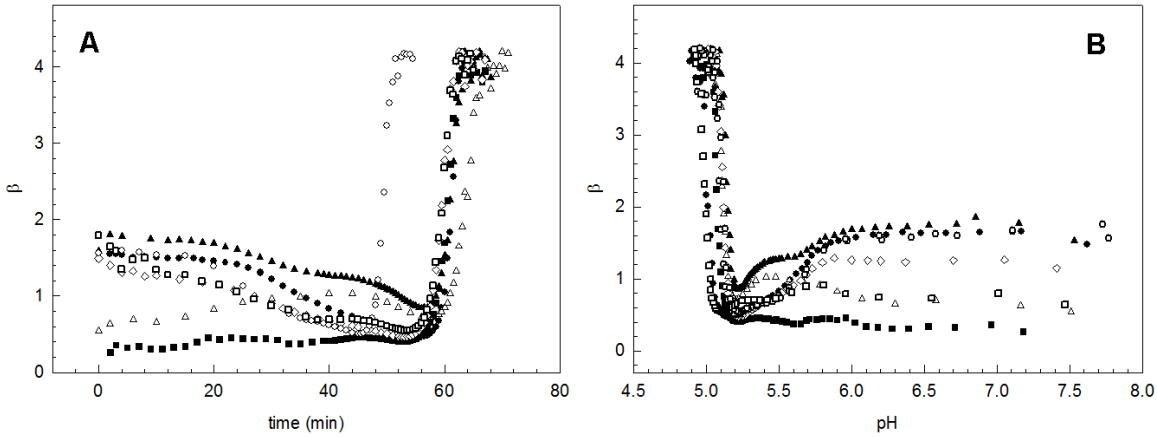


**Fig. 5:** Variations of parameter β, proportional to the average size of particles, as a function of time (A) and pH (B), after glucono-δ-lactone (GDL) addition, during the acid aggregation of NaCAS:hydrolysates mixtures (4:1): NaCAS without hydrolysate (○), with $t_0$ (●), with $t_1$ (Δ), with $t_2$ (▲), with $t_3$ (□), with $t_4$ (■), and with $t_7$ (◊), where the subscript i correspond to the hydrolysis time. Assays performed at 35ºC; GDL mass fraction/protein mass fraction (R) = 0.5; NaCAS:hydrolysates total concentration = 5 mg $g^{-1}$.

**Figure 6**

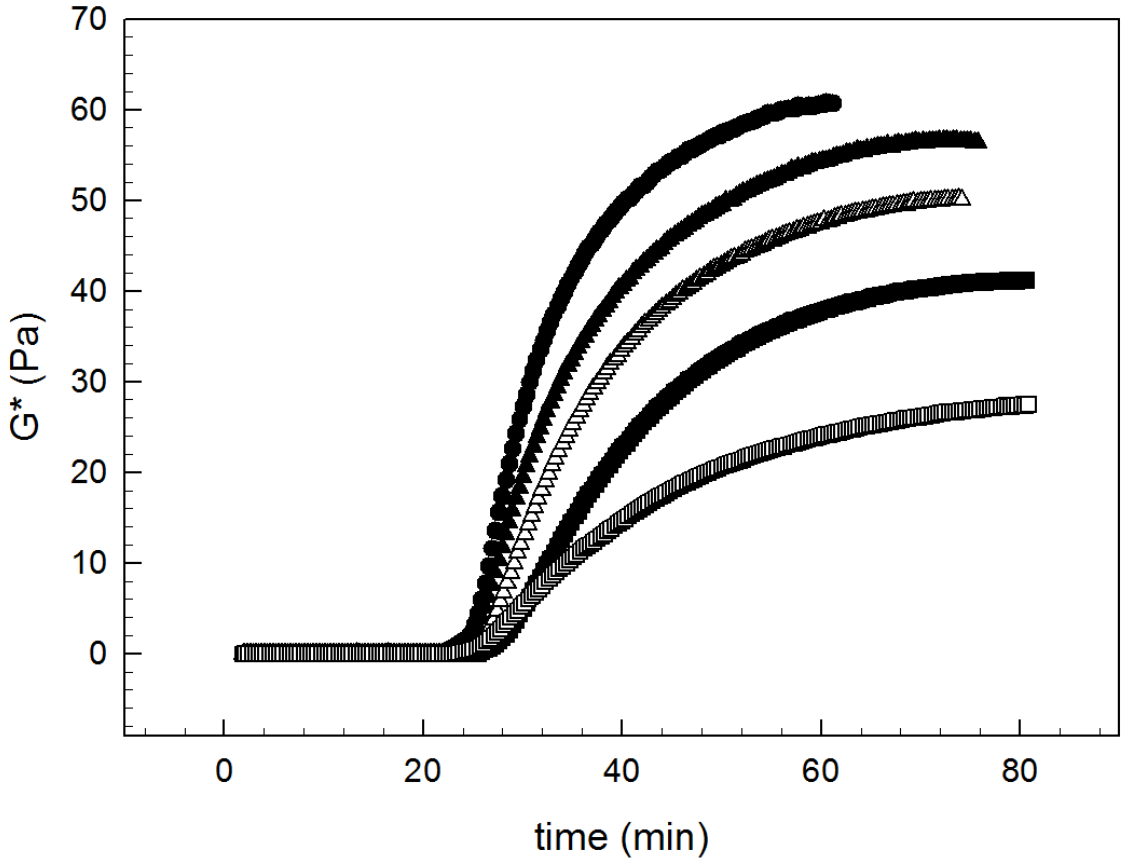


**Fig. 6:** Time dependence of the complex modulus G* (at 0.1 Hz) for NaCAS:hydrolysates mixtures (4:1) acid gels obtained at different hydrolysis times ($t_i$): NaCAS:hydrolysate $t_i$: $t_0$ (●), $t_1$ (Δ),$t_2$ (▲), $t_3$ (□), $t_4$ (■), where the subscript i correspond to the hydrolysis time. NaCAS concentration: 30 mg $g^{-1}$, hydrolysate concentration: 7.5 mg $g^{-1}$, R = 0.5 and T = 35 ºC.

**Figure 7**

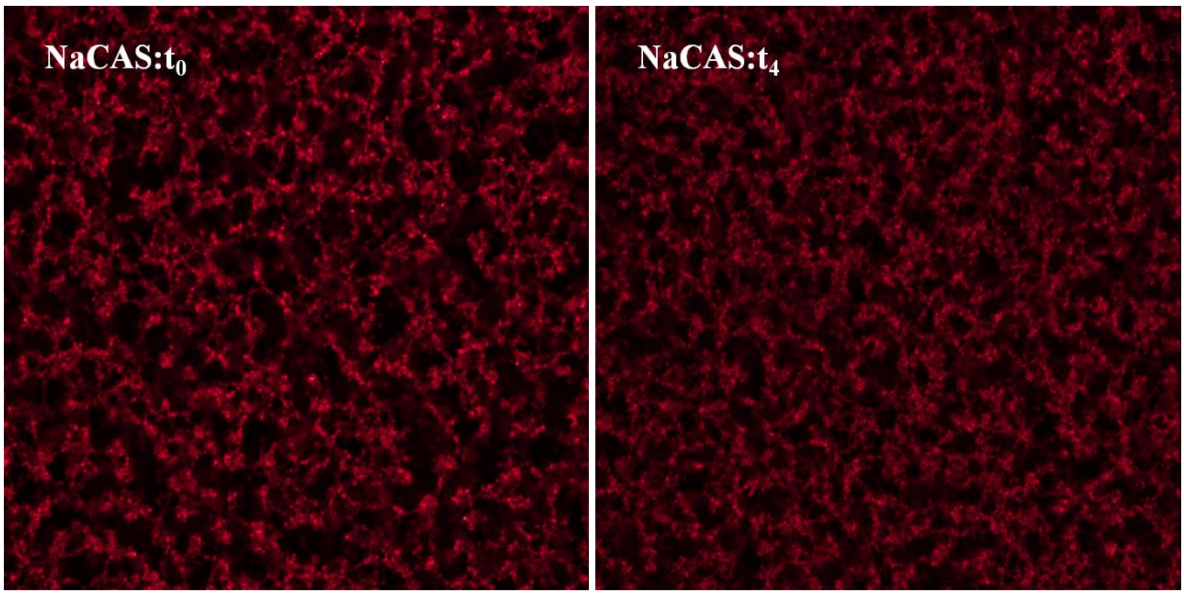


**Fig. 7:** Microphotographs of NaCAS:hydrolysates $t_0$ and $t_4$ gels obtained by CLSM, using Rhodamine B ($2 \times 10^{-3}$ mg $mL^{-1}$). NaCAS concentration: 30 mg $g^{-1}$, hydrolysate concentration: 7.5 mg $g^{-1}$, R = 0.5 and T = 35 ºC.

**Figure 8**

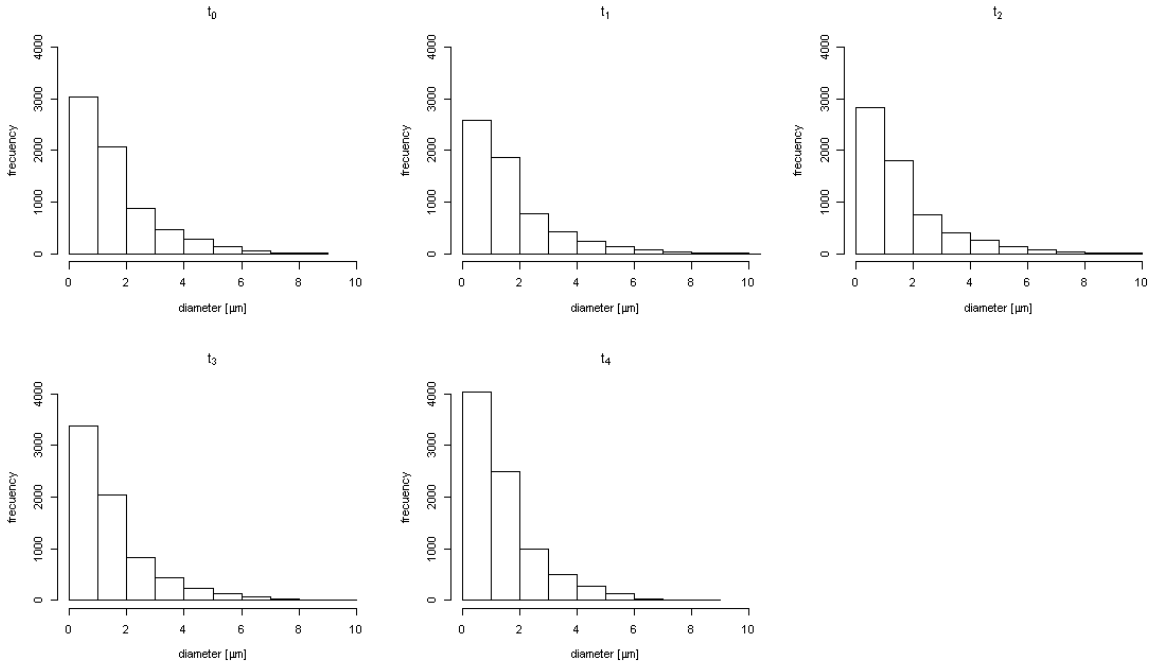


**Fig. 8:** Pore diameter distribution of NaCAS:hydrolysates gels obtained by addition of GDL at 35°C. NaCAS concentration: 30 mg $g^{-1}$, hydrolysate concentration: 7.5 mg $g^{-1}$, R = 0.5.

Highlights:

- Biological activities of sodium caseinate hydrolysates were observed
- Peptides from bovine $\alpha_{S1}$-CN and β-CN were identified
- Bioactive peptides did not aggregate under acid conditions
- Incorporation of hydrolysates modifies the kinetics of the acid aggregation process
- Hydrolysates alter the microstructure and rheological behavior of acid gels

**Table 1**

Antioxidant activities of the hydrolysates of NaCAS obtained by hydrolysis with P7PP

| Hydrolysis time (h) | ABTS radical scavenging activity (%) | $Fe^{2+}$- chelating ability (%) | Reducing power (Absorbance at 700 nm) |
|---|---|---|---|
| 0 | 52.60 ± 0.08[a] | 78.400 ± 0.005[a] | 0.106 ± 0.007[a] |
| 0.5 | 59.5 ± 0.1 | 89.800 ± 0.003 | 0.133 ± 0.002 |
| 1 | 70.20 ± 0.02 | 93.40 ± 0.02 | 0.171 ± 0.005 |
| 2 | 67.90 ± 0.05 | 93.300 ± 0.008 | 0.22 ± 0.03 |
| 3 | 71.20 ± 0.02 | 94.60 ± 0.04 | 0.30 ± 0.01 |
| 4 | 74.100 ± 0.008 | 80.300 ± 0.004 | 0.25 ± 0.01 |
| 6 | 75.30 ± 0.01 | 91.200 ± 0.005 | 0.262 ± 0.004 |

[a] Mean value ± standard deviation ($p < 0.05$)

**Table 2**

Antimicrobial activities of the hydrolysates obtained by hydrolysis of NaCAS with P7PP

| **Indicador microorganism** | **Inhibition zone (mm)**[a] | |
|---|---|---|
| **Hydrolysis time (h)** | **0.5** | **1.0** |
| **Gram-positive bacteria** | | |
| *Listeria monocytogenes* ATCC 15131 | 8.0 | 10.0 |
| *Bacillus cereus* ATCC 9634 | -[b] | |
| *Corynebacterium fimi* NCTC 7547 | 7.0 | 10.0 |
| *Staphylococcus aureus* ATCC 1901 | - | |
| **Gram-negative bacteria** | | |
| *Salmonella enteritidis* ATCC 13076 | 8.0 | 11.0 |
| *Escherichia coli* ATCC 8739 | 6.0 | 9.0 |

[a] Values for haloes are the means of three independent determinations.
[b] Without inhibition.

**Table 3**

Values of fractal dimension ($D_f$) of NaCAS:hydrolysates mixtures (4:1), $t_i$ = hydrolysis time (h). NaCAS concentration 5 mg $mL^{-1}$, hydrolysates concentration 1.25 mg $mL^{-1}$, glucono-δ-lactone mass fraction/protein mass fraction (R) 0.5 and T 35ºC.

| System | $D_f \pm 0.02$[a] |
|---|---|
| NaCAS without hydrolysis | 4.17 |
| NaCAS: $t_0$ | 4.14 |
| NaCAS: $t_1$ | 4.16 |
| NaCAS: $t_2$ | 4.18 |
| NaCAS: $t_3$ | 4.17 |
| NaCAS: $t_4$ | 4.18 |

[a] Mean value ± standard deviation ($p < 0.05$)

**Table 4**

The steady-state value of the complex shear modulus ($G^*_{eq}$) and the initial rate of increase in G* (k) for NaCAS:hydrolysates mixtures acid gels (4:1) obtained at different hydrolysis times ($t_i$). NaCAS concentration: 30 mg $g^{-1}$, hydrolysates concentration: 7.5 mg $g^{-1}$, R = 0.5 and T = 35 ºC.

| $t_i$ | $G^*_{eq}$ (Pa) | k ($min^{-1}$) |
|---|---|---|
| $t_0$ | 61.4 ± 0.1[a] | 0.1105 ± 0.0008 |
| $t_1$ | 57.60 ± 0.08 | 0.0809 ± 0.0005 |
| $t_2$ | 51.59 ± 0.04 | 0.0751 ± 0.0002 |
| $t_3$ | 43.16 ± 0.08 | 0.0645 ± 0.0004 |
| $t_4$ | 29.56 ± 0.04 | 0.0488 ± 0.0002 |

[a] Mean value ± standard deviation ($p < 0.05$)

**Table 5**

Mean pore diameters and pore area of acid gels obtained from NaCAS:hydrolysates $t_i$ mixtures (30 mg $g^{-1}$ : 7.5 mg $g^{-1}$), where $t_i$ is the hydrolysis time. Ratio GDL/NaCAS concentrations (R) = 0.5 and T = 35ºC.

| NaCAS: hydrolysates $t_i$ mixtures | Mean pore diameter[a] (μm) | Pore area[a] (μm) | Homogeneous group[b] |
|---|---|---|---|
| $t_0$ | 1.659 ± 0.021 | 3.519 ± 0.109 | BC |
| $t_1$ | 1.733 ± 0.035 | 4.027 ± 0.211 | C |
| $t_2$ | 1.678 ± 0.025 | 3.750 ± 0.138 | BC |
| $t_3$ | 1.591 ± 0.023 | 3.334 ± 0.126 | AB |
| $t_4$ | 1.521 ± 0.014 | 2.862 ± 0.083 | A |

[a] Mean value ± standard deviation ($p < 0.05$)

[b] Different letters denote mean value of mean pore diameter and pore area parameters significantly different among the values of $t_i$ (A stands for the lowest, B for medium value and C for the highest value, respectively)

**Table 6**

Textural parameters obtained from digital images of NaCAS:hydrolysate acid gels in function of hydrolysis time ($t_i$): Shannon entropy (*S*), smoothness (*K*), uniformity (*U*), and mean normalized grey-level variance ($\sigma^2(N)$). NaCAS concentration: 30 mg $g^{-1}$, hydrolysate concentration: 7.5 mg $g^{-1}$, R = 0.5 and T = 35 ºC.

| $t_i$ | *S* | *K* (x $10^{-3}$) | *U* (x $10^{-3}$) | $\sigma^2(N)$ | ANOVA for *S* | ANOVA for *K* | ANOVA for *U* | ANOVA for $\sigma^2(N)$ |
|---|---|---|---|---|---|---|---|---|
| $t_0$ | 5.02±0.03[a] | 3.67±0.17 | 39.43±0.97 | 239.48±10.93 | A[b] | A | C | A |
| $t_1$ | 5.26±0.02 | 4.76±0.12 | 32.95±0.48 | 310.80±7.82 | B | C | B | AB |
| $t_2$ | 5.24±0.03 | 4.43±0.22 | 32.81±0.70 | 289.04±14.38 | B | BC | B | AB |
| $t_3$ | 5.43±0.04 | 4.97±0.26 | 27.96±0.88 | 325.04±17.22 | B | C | A | B |
| $t_4$ | 5.29±0.02 | 4.09±0.09 | 30.20±0.40 | 266.95±6.02 | B | AB | AB | AB |

[a] Mean value ± standard deviation ($p < 0.05$)

[b] Different letters denote mean value of parameter *K*, *S*, *U*, $\sigma^2(N)$ significantly different among the values of $t_i$ (A stands for the lowest, B for medium value and C for the highest value, respectively)